Universal law for piecewise dimer diffusion

F. Montalenti* and R. Ferrando†
INFM and CFSBT/CNR, Dipartimento di Fisica dell'Università di Genova, via Dodecaneso 33, 16146 Genova, Italy
(Received 23 February 1999; revised manuscript received 29 April 1999)

We present a theoretical study of the dissociation-reassociation (DR) mechanism for one-dimensional dimer diffusion. Through a random-walk calculation we find an exact analytical expression for the jump-length ($|l|$) probability distribution $P(|l|)$, and we show that such a distribution is very well approximated, already for small $|l|$ ($|l| \gtrsim 3$), by its simple asymptotic form $P(|l|)=1/(\pi|l|^2)$. We derive the exact expression of the time-dependent probability distribution $\Phi(l,t)$, a quantity which is usually measured in scanning tunneling microscopy and field-ion microscopy experiments, both in the case in which the dimer diffuses only by the DR mechanism and in the case in which other mechanisms (such as the concerted jump and the leapfrog) are possible. This expression is useful in fitting the experimental data. Theoretical and experimental consequences are discussed. [S0163-1829(99)03239-7]

I. INTRODUCTION

The knowledge of the single-adatom surface-diffusion mechanisms and energetics is the starting point for more ambitious studies of fundamental technological interest such as thin film and crystal growth.[1] Thanks to a great amount of literature (mainly concentrated in the last decade) the single-adatom problem for a wide set of surface geometries and chemical species is now deeply investigated. Still, it is sufficient to consider the smallest cluster, the dimer, in order to find some important questions which are still open. Indeed, the role that dimer diffusion plays in growth processes is not yet fully understood.[2]

Recently, dimer surface diffusion has attracted a considerable attention because new diffusion mechanisms were experimentally discovered and theoretically investigated, both on metal and on semiconductor surfaces. Indeed, in a scanning tunneling microscopy (STM) experiment, Borovsky, Krueger, and Ganz[3] discovered a new diffusion path for the silicon dimer on Si(001); this mechanism has been theoretically investigated in a subsequent paper by Goringe and Bowler.[4] Concerning metals, Linderoth *et al.*,[5] again by STM, found evidence for a novel diffusion mechanism in $Pt_n/Pt(110)(1\times2)(n\geqslant3)$, called leapfrog (LF). The present authors showed[6] that this mechanism is present not only in long-chain diffusion, but also in dimer diffusion, and that it seems to be a common feature of metal dimer diffusion on $(110)(1\times2)$ surfaces.[7]

In the case of dimer diffusion, the breakup of the dimer into two isolated adatoms (i.e., the dissociation process) must be considered. Experimental[2,8–10] and theoretical[7,11–13] results showed different behaviors depending on the chemistry and on the geometry of the systems: dissociation seems to be favorite with respect to other dimer diffusion mechanisms in $Pt_2/Pt(110)(1\times2)$,[8] $Al_2/Al(110)$,[11] and $Cu_2/Au(110)(1\times2)$,[7] while in $Pt_2/Pt(111)$,[2,12] $W_2/W(110)$,[9,10,13] AuCu/Au(110)(1×2), and $Au_2/Au(110)(1\times2)$ (Ref. 7) other processes seem to be easier than dissociation. In all the above-mentioned systems, however, the activation barrier for dissociation is higher than the single-adatom diffusion barrier. Therefore, after dissociation, the two adatoms move on a much shorter time scale than the average time between breakup events, until they reassociate again. Thus, as very recently observed by Borovsky, Krueger, and Ganz,[14] typical atom-tracking data, at suitable temperatures, would only reveal dimer motion. Hence such a dissociation-reassociation (DR) mechanism should be considered as an effective *piecewise* dimer diffusion mechanism, giving rise to *effective dimer long jumps*.

In this paper we derive the exact expression for the jump-length probability distribution $P(|l|)$ for a dimer diffusing by the DR mechanism in one dimension. We show that $P(|l|)$ decays slowly with the length l [$P(|l|)\propto l^{-2}$], so that dimer diffusion by the DR mechanism is dominated by effective long jumps. Then we derive an exact expression for the time-dependent probability density $\Phi(l,t)$. The latter quantity is usually measured in STM and in field-ion microscopy (FIM) experiments. Our expression for $\Phi(l,t)$ contains a single parameter (the dissociation rate of the dimer); therefore a fitting of the experimental data by means of our formula would lead to the determination of the dissociation rate, and an Arrhenius plot of this rate would give the dissociation barrier and prefactor. We consider also the case in which other mechanisms are possible besides DR, and show that the behavior of $\Phi(l,t)$ depends strongly on the competition between DR and the other mechanisms. In the case of the presence of a single mechanism besides DR [as it happens, for example, in fcc(110) unreconstructed surfaces, where DR and concerted jumps (CJ) are possible], we show that $\Phi(l,t)$ depends on two parameters, the dissociation rate itself and the ratio between the dissociation rate and the rate of the other mechanism. A fitting of $\Phi(l,t)$ would thus lead to the determination of both rates.

The paper is organized as follows. In Sec. II we derive the exact analytical expression for the effective long-jump distribution $P(l)$ (l is an integer) induced by the DR mechanism in one dimension, and study its asymptotic behavior. In Sec. III we calculate the time-dependent probability distribution. In Sec. IV the finite-size effects, caused by the finite extension of the terraces on the surface, are discussed with the aid of kinetic Monte Carlo simulations. In Sec. V we

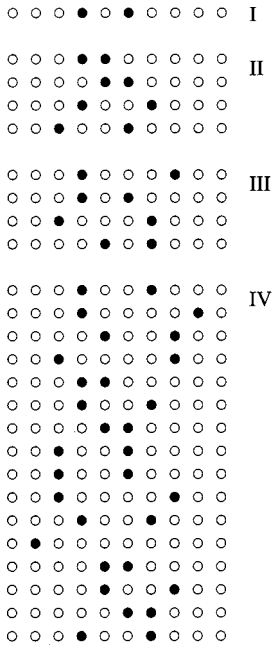

FIG. 1. All possible configurations reachable by the two adatoms (full black circles) in the first four steps or their random walk. When the dimer reassociates, the corresponding configuration is removed.

consider the diffusion of dimers in real systems, where other dimer diffusion mechanisms are competing with DR. Section VI contains the conclusions.

II. UNIVERSAL LAW FOR PIECEWISE DIMER DIFFUSION IN ONE DIMENSION

Let us consider the following problem: a dimer is deposited on a metal surface where diffusion, for both the dimer and the single adatom, is mainly a one-dimensional process. Channeled surfaces where both out-of-channel jumps and exchanges are unlikely (for both adatoms and dimers) are among the systems which satisfy this requirement. Our aim is to calculate the dimer jump-length probability distribution $P(l)$ which is induced by the DR mechanism. We note that the other possible dimer diffusion mechanisms (for example, the concerted jump and the leapfrog) cause only one-site moves (i.e., single jumps), whereas the DR mechanism can cause, in principle, jumps of any length (see below).

In order to calculate $P(l)$, we assume that the dimer dissociates at time step 0, so that at time step 1 we have two separated adatoms with one empty cell in between. In the following steps one-site moves of one of the two adatoms take place. If the two adatoms reassociate again, thus recreating a dimer, we consider this situation stable, i.e., the adatoms remain fixed in such position. Note that, on a suitable time scale, this assumption is realistic since dissociation is usually a much slower process with respect to the single-adatom moves. The configuration space for the first four steps is displayed in Fig. 1. Of course, reassociation is possible only in an even number $2m$ of steps. If a is the nearest-neighbor distance, and if the dimer center of mass is in $a/2$ at step 0, we ask which is the probability $P(l)$ of finding the dimer reassociated l sites away [with its center of mass in $(l+1/2)a$]. $P(l)$ is given by

$$P(l)=\sum_{m=l}^{\infty} Q(2m)p(2m,l), \tag{1}$$

where $p(2m,l)$ is the probability the two adatoms have to meet each other for the first time in the position l after $2m$ steps. In the following, we define a *2m random walk* as a random walk during which the two adatoms do not reassociate for the first $2m-1$ steps and they do associate exactly at the $2m$th step. $Q(2m)$ is the probability for the two adatoms to perform such a random walk. Now we calculate $p(2m,l)$ and $Q(2m)$ independently. First, we consider $Q(2m)$. While the dimer is dissociated, the relative coordinate $x_r=x_2-x_1-1$ of the two adatoms takes randomly positive values, starting from the value 0. At the reassociation, x_r returns back to 0. Therefore, this problem is mapped exactly onto the problem of the first return to the origin of a single unbiased random walker in one dimension. This problem has been exactly solved a long time ago, and we omit any detail (the latter can be found, for example, in Refs. 15 and 16). In one dimension, the random walker comes back to its original position with probability 1 (Polya's theorem, for example, see Ref. 15). $Q(2m)$ reads

$$Q(2m)=\binom{2m}{m}\left(\frac{1}{4}\right)^m \frac{1}{(2m-1)}. \tag{2}$$

$Q(2m)$ is the correct weight for a $2m$ random walk; now we look for the probability that the final reassociation occurs l sites away from the initial position, i.e., we concentrate on $p(2m,l)$. Let us consider the evolution of the center-of-mass coordinate X_G in a $2m$ random walk. We indicate with R and L the number of right and left moves of X_G, respectively, with $R+L=2m$. The total displacement of X_G is $n=R-L$. Since the adatoms have the same probability of jumping to the right or to the left, the probability of a $2m$ random walk with R moves to the right and L to the left, is simply

$$p(2m,R,L)=\frac{(2m)!}{R!L!}\left(\frac{1}{2}\right)^{2m}. \tag{3}$$

R and L must be both even or both odd, which gives an n always even. The displacement of X_G is given by the integer $l=n/2$, and $p(2m,l)$ is given by

$$p(2m,l)=\frac{(2m)!}{(m-l)!(m+l)!}\left(\frac{1}{2}\right)^{2m}. \tag{4}$$

Finally, substituting in Eq. (1)

$$P(l)=\sum_{m=l}^{\infty}{}'\binom{2m}{m}\left(\frac{1}{4}\right)^{2m}\frac{1}{(2m-1)}\frac{(2m)!}{(m-l)!(m+l)!}, \tag{5}$$

where Σ' indicates that the sum starts from $m=1$ when $l=0$. In our derivation, the evolution of X_G has been treated as a simple unbiased random walks. This *modus operandi* may appear obvious, but it must be used with care (for example, it is wrong in two or three dimensions). Indeed, the evolution of X_G during a $2m$ random walk is a constrained random walk. For example, let us consider a 2 random walk: after one step, the two adatoms are separated by one empty site. If there was no constraint, at the second step, they could reach anyone of the four configurations displayed in Fig. 1

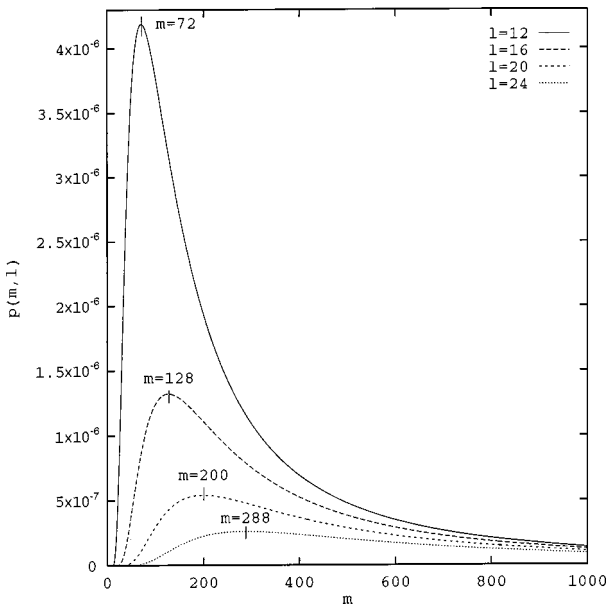

FIG. 2. $p(m,l)$ computed from Eq. (4), for four typical large l values. Note that the maxima correspond to $m=l^2/2$.

(II). Without constraint, X_G has the same probability (1/2) to make a left or a right move at step 2. But in a 2 random walk only the two moves leading to reassociation are allowed, so that a constraint effectively acts by excluding some configurations. Still, by weighting only on the allowed configurations, it is again true that X_G moves to the right or to the left with probability 1/2. It is straightforward to verify that, also for $m>2$, such constraint does not influence the X_G motion, which can be correctly treated as a simple unbiased random walk. On the contrary, for two-dimensional walkers, the constraint does not allow us to treat X_G as a simple unbiased random walk.

Let us now inspect, with the aid of Eq. (5), the asymptotic behavior of $P(l)$ for large values of l. The key observation is that all the factorials in Eq. (5) are much greater than 1 in this limit. Indeed, for every large l, only terms with $m \gg l$ contribute to $P(l)$ since the probability of reassociating l sites away in a number of steps close to l is extremely small. Simple random-walk considerations suggest that a final displacement l is likely to be reached by $2m \approx l^2$ steps, as confirmed by solving numerically Eq. (5) (see Fig. 2). Hence also $(m-l)! \gg 1$ and if we consider Eq. (5) with $n=m-l$

$$P(l)=\sum_{n=0}^{\infty}\frac{[2(l+n)]![2(l+n)]!}{(l+n)!(l+n)!n!(n+2l)!}\times\left(\frac{1}{4}\right)^{2(l+n)}\frac{1}{2l+2n-1}, \tag{6}$$

we can replace all the factorials in Eq. (6) by using the Stirling approximation $(l! \to \exp(-l)(2\pi l)^{1/2}l^l)$. A simple calculation gives

$$P(l)\to\frac{1}{\pi}\sum_{n=1}^{\infty}\frac{(l+n)^{2(l+n)}}{n^n(2l+n)^{(2l+n)}}\times\{[n(n+2l)](2l+2n-1)^2\}^{-1/2}. \tag{7}$$

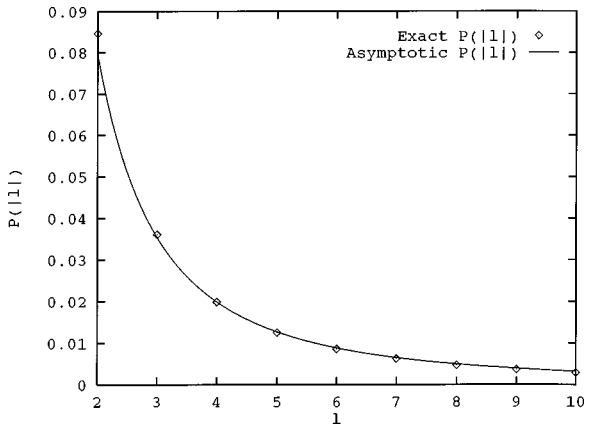

FIG. 3. Exact probability jump-length distribution $P(|l|)$ (diamonds) given by Eq. (5) compared with its asymptotic behavior $1/(\pi|l|^2)$ (solid line). Only for $l>3$, significant differences can be noted.

By making an expansion in powers of l/n, after some calculations one has

$$P(l)\to\frac{1}{2\pi}\int_1^{\infty}\exp\left(\frac{-l^2}{x}\right)\frac{dx}{x^2}\approx\frac{1}{2\pi l^2}. \tag{8}$$

Since for every $l \geqslant 1$, $P(|l|)=2P(l)$, we obtain the final result

$$\lim_{l\to\infty}P(|l|)=\frac{1}{\pi l^2}. \tag{9}$$

This result shows that the DR mechanism causes a jump-length distribution $P(|l|)$ which slowly decays with $|l|$. We recall that, concerning adatoms diffusion, the occurrence of double jumps have been experimentally demonstrated for different systems such as Ir/W(110),[17] Na/Cu(100),[18] Pd/W(211),[19] and Pt/Pt(110)(1×2).[20] In some of these systems, an indication of the role played by triple jumps was given too, but longer jumps could not be analyzed in a systematic way, as well as in many molecular-dynamics (MD) simulations (see Refs. 21 and 22). This was due to the lack of longer-jump statistics, because of the quick decay (exponential, see Refs. 23–25) of the single-adatom jump-length probability distribution. On the other hand, dimers can be an ideal system in order to detect long jumps. Indeed, very recently, Borovsky, Krueger, and Ganz[14] could easily observe in their atom-tracking data on $Si_2/Si(001)$ effective triple jumps induced by the DR mechanism.

In Fig. 3 the exact $P(|l|)$, as numerically calculated from Eq. (5), is compared with its asymptotic limit. The extremely simple law given by Eq.(9) gives a very good approximation for the $P(|l|)$ already for $l \gtrsim 3$. The results shown in Fig. 3 and Table I are in fairly good agreement with those of Goringe and Bowler.[4] These authors calculated numerically $P(l)$, without giving the exact analytical expression. Small differences [from our exact results, the 67% of the effective jumps $(|l|>0)$ cause a one-site move, while they find a higher percentage, 71%] may be due to some lack of accuracy in their numerical calculations.

TABLE I. Exact values for $P(|l|)$ computed from Eq. (5), normalized on all DR events (second column), and on nonzero displacements (third column).

$\|l\|$	$P(\|l\|)$	$P^*(l)=P(\|l\|)/[1-P(0)]$
0	0.3632	
1	0.4241	0.666
2	0.0846	0.133
3	0.0360	0.056
4	0.0199	0.031
5	0.0125	0.020
6	0.0086	0.013

The slow decay of $P(l)$ has important consequences. As obvious, all the moments will diverge, and in particular:

$$\langle l^2\rangle=\sum_l P(l)l^2=\infty. \tag{10}$$

Does this mean that the DR mechanism forces dimers diffusion to be anomalous? Clearly, the answer is negative. Without some care in the interpretation of our results, a paradox would be produced. Indeed all dimer-diffusion barriers are higher than the single adatom one, while following Eq. (10), dimers diffusion coefficient would be larger (infinite) than the adatom one. The answer to such paradox resides in the approximation we used to model dimer diffusion, and to find the general form for $P(l)$ [Eq. (5)]. In particular, we neglected the time spent while the dimer is dissociated. This is a good approximation until the number of adatom moves is much less than the ratio between the dimer and the adatom time scale. Let us clarify this point with an example. Au_2 diffusion on $Au(110)(1\times2)$ is a good example of a system where the hypothesis for Eq. (5) is satisfied. In such a system, following our calculations of Ref. 6, the single-adatom barrier is $E_j=0.31$ eV, while the dominant diffusion mechanism is leap-frog, with a barrier of $E_{LF}=0.45eV$. So, for single-adatom diffusion, the typical time-scale τ_{ad} is given by $\nu_{ad}^{-1}\exp(E_j/k_BT)$, while for dimers $\tau_{dim}=\nu_{dim}^{-1}\exp(E_{LF}/k_BT)$. Assuming equal prefactors, the ratio between the two time scales is at room temperature

$$\frac{\tau_{dim}}{\tau_{ad}}\approx 220. \tag{11}$$

Since the most important contributions to $P(l)$ come from single-adatom random walks of length of $\approx l^2$ steps, neglecting the time spent while the dimer is dissociated is wrong for $l\gtrsim 15$.

III. TIME-DEPENDENT PROBABILITY DISTRIBUTION

Let us construct the time-dependent probability distribution $\Phi(l,t)$ (the probability of being at site l at time t starting from the origin at time zero) for the dimer. Such observable quantity is of main interest, since one of the experimental ways to investigate the long-jump distribution is to carry on a final displacement analysis (for example, see Ref. 20).The problem of finding $\Phi(l,t)$ for a dimer diffusing in one dimension was considered in some pioneering works by Ehrlich and co-workers.[26,27] In these papers diffusion on adjacent channels on $W(211)$-like surfaces was investigated. Though the geometry here considered is different (diffusion occurs in only one channel), the theoretical treatment is the same.

The master equation for a one-dimensional random walker making jumps of any length with a jump-length probability distribution $P(k)$ is given by

$$\frac{d}{dt}\Phi(l,t)=r\sum_{k=-\infty}^{\infty}P(k)\{\Phi(l+k,t)-\Phi(l,t)\}, \tag{12}$$

where r is the total jump rate (in the case of the DR mechanism r is the dissociation rate ν_{Di}). Multiplying both members of (12) by e^{iql}, and summing over l, one obtains

$$\frac{d}{dt}\Phi(q,t)=r\sum_{k=-\infty}^{\infty}P(k)\Phi(q,t)\{e^{-iqk}-1\}. \tag{13}$$

In Eq. (13) we introduced the Fourier transform $\Phi(q,t)=\Sigma_l e^{iql}\Phi(l,t)$. From Eq. (13), if the initial condition $\Phi(l,0)=\delta_{l,0}$ is imposed, it follows immediately:

$$\Phi(q,t)=e^{-f(q)t}, \tag{14}$$

where

$$f(q)=r\sum_k P(k)\{1-e^{-iqk}\}=r\sum_{k>0}P(|k|)\{1-\cos(qk)\}, \tag{15}$$

and $P(|k|)=P(k)+P(-k)$. By taking the inverse Fourier transform of Eq. (14), one finally obtains

$$\Phi(l,t)=\frac{1}{2\pi}\int_0^{2\pi}\cos(ql)\times\exp\left(-rt\sum_{k>0}\{1-\cos(qk)\}P(|k|)\right)dq. \tag{16}$$

With some calculations, it is possible to write Eq. (16) in a different way. Let us assume that only single jumps are possible. Thus $P(1)=1$, and $P(k)=0$, $k\neq 1$. Hence we find the well-known formula

$$\Phi_1(l,t)=e^{-r_1t}I_l(r_1t), \tag{17}$$

where we introduced the modified Bessel functions

$$I_l(r_jt)=\frac{1}{2\pi}\int_0^{2\pi}\cos(ql)e^{r_jt\cos(q)}dq. \tag{18}$$

It is straightforward to verify that, if only jumps of length n are allowed, then

$$\Phi_n(nl,t)=e^{-tr_n}I_l(r_jt). \tag{19}$$

As in Eqs. (17) and (19), in the following we shall indicate with Φ_n the time-dependent probability distribution for a system where only jumps of n cells are allowed, and r_n is the corresponding jump rate. Let us now consider a system where both single and double jumps are possible. We may ask what is the probability of being in l at the time t, starting

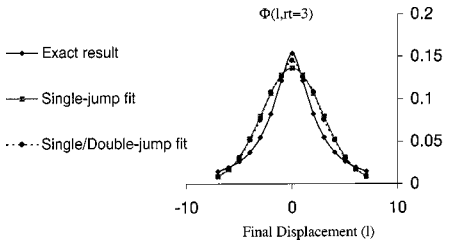

FIG. 4. $\Phi(l,t)$ for $rt=3$ (black solid line + diamonds), compared with single-jump (gray solid line + squares) and single- and/or double-jump (black dashed line + circles) probability distribution best fits. Both fits are clearly poor.

from the origin at the time 0. We divide the real walk into all possible couples of subwalks made of $(l-2n)$ single jumps only and of $(2n)$ double jumps only. Each of such couples would give a contribution to $\Phi(l,t)$:

$$\tilde{\Phi}(l,t)=P_1(l-2n,t)P_2(2n,t). \tag{20}$$

By summing over all possible walks of this kind, and using Eq. (19), one obtains for such single- and double-jump probability distributions[28,29]

$$\Phi(l,t)=e^{-t(r_1+r_2)}\sum_{n=-\infty}^{\infty} I_{l-2n}(r_1t)I_n(r_2t). \tag{21}$$

By repeating our walk division into sets of subwalks composed by jumps of a given length, it should be straightforward for the reader to verify that, if jumps of any length are allowed, then

$$\Phi(l,t) = e^{-tr}\sum_{n2,n3,\ldots=-\infty}^{\infty} I_{l-\sum_{j=2}^{\infty} jn_j}(rP(1)t)\prod_{k=2}^{\infty} I_{n_k}(rP(k)t), \tag{22}$$

where $r=\Sigma_j r_j$ is the total jump rate.

A method used by the experimentalists to detect long jumps (see again Ref. 20) is to fit the displacements distribution $\Phi(l,t)$ at a given time t with Eq. (22), allowing only jumps of a maximum length (typically only single jumps or single and double jumps are considered since longer-jump statistics is poor). In Fig. 4, we show $\Phi(l,t)$ calculated from Eq. (16) with $P(k)$ given by Eq. (5), in a typical experimental situation $(rt=3)$, together with a single-jump probability-distribution fit and a single- and double-jump probability-distribution fit. The fit turns out to be poor in both cases, even if a certain improvement is achieved allowing double jumps.

In systems where DR is the dominant dimer-diffusion mechanism, Eqs. (16) and (22) can be used in the analysis of the experimental data, to extract from them the dissociation rate ν_{Di} by fitting the single parameter r of the distribution. An Arrhenius plot of ν_{Di} would then give the dissociation barrier and prefactor. The case of systems where other mechanisms compete with DR is treated in Sec. IV.

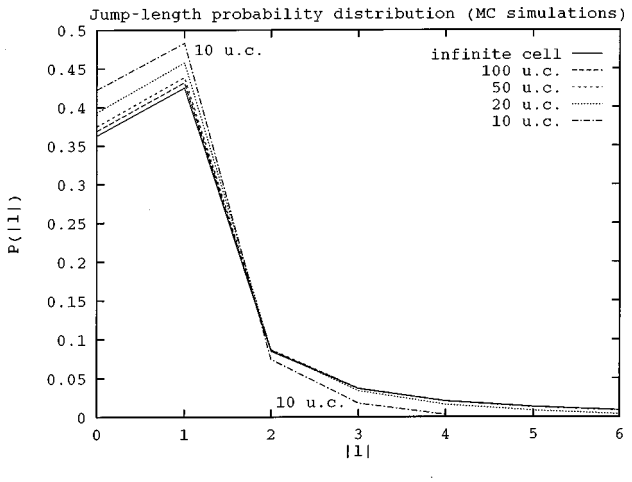

FIG. 5. $P(|l|)$ extracted from MC simulations of dimer diffusion on finite lattices. Only for the extremely small 10-unit-cells (u.c.) lattice, deviations from the infinite lattice are significant. In this figure we did not show the exact values given by Eq. (5), since they are perfectly reproduced by the MC simulation for the infinite lattice.

IV. FINITE-SIZE EFFECTS

In the preceding sections the two adatoms were left free to move in an infinite lattice. Of course this is not the case in a typical experiment, where terraces, steps, other small clusters, and isolated adatoms are present. If one of the dimer adatoms meets a defect during its random walk, it will be captured by the defect. In order to study the typical effect of a finite lattice on the universal long-jump distribution $P(|l|)$, we performed a set of Monte Carlo (MC) simulations. In such simulations, in the initial position the two adatoms are separated by one lattice spacing, and at every step one of them jumps either to the left or to the right. The simulation ends when the two adatoms are in the dimer configuration or when one of them reaches the lattice boundaries. In Fig. 5 results for an infinite lattice are compared with lattices composed by 100, 50, 20, and 10 sites. For every lattice, $P(|l|)$ is calculated by averaging over 10^6 simulations. As it can be easily seen, only in the 10-site lattice $P(|l|)$ is significantly affected by finite-size effects. However, much larger clean terraces can be obtained by the experimentalists. For all other lattices, in a relevant range of jump lengths, $P(|l|)$ extracted from MC simulations does not deviate significantly from the values given by Eq. (5).

V. THE JUMP-LENGTH PROBABILITY DISTRIBUTION IN REAL SYSTEMS

Equation (16) gives the jump-length probability distribution $P(l)$ induced by the DR mechanism. This probability distribution is universal since we found it under very general hypothesis. Very often, in real systems, other dimer-diffusion mechanisms must be taken into account too. Let us calculate the explicit form of the probability distributions for a real system, where piecewise diffusion is in competition with another diffusion mechanism (*mech* in the following), for example CJ or LF. As we already remarked, all known diffusion mechanisms (except DR) for one-dimensional dimer diffusion cause single-site moves. The frequency

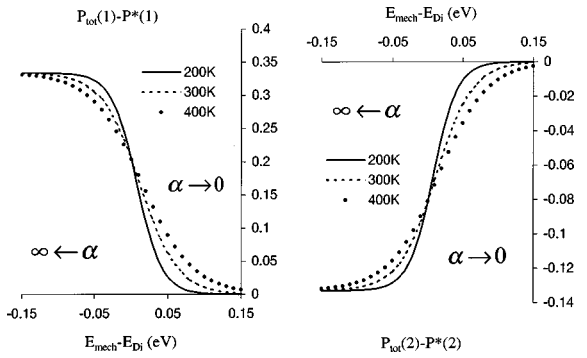

FIG. 6. Deviations of $P_{tot}(1)$ (left) and $P_{tot}(2)$ (right) as a function of $E_{mech}-E_{Di}$ for three different temperatures. When *mech* becomes dominant ($\alpha\to\infty$), $P_{tot}(1)\to 1$ [and $P_{tot}(1)-P^*(1)\to 1-P^*(1)\approx 0.33$] and $P_{tot}(2)\to 0$, since the single-jump contribution becomes fully dominant. On the other hand, if DR dominates ($\alpha\to 0$), the universal behavior is quickly reached. For $k\geqslant 3$, $P_{tot}(k)$ displays the same qualitative behavior of $P_{tot}(2)$. The curves have been computed by assuming equal prefactors for DR and *mech*.

ν_{mech} of the *mech* mechanism is given by the Arrhenius form

$$\nu_{mech}=\nu^0_{mech}\exp(-E_{mech}/k_BT), \tag{23}$$

where k_B is the Boltzmann constant, E_{mech} is the activation barrier for the *mech* process, and ν^0_{mech} its frequency prefactor. The frequency ν_{Di} of the DR mechanism follows an Arrhenius form as well

$$\nu_{Di}=\nu^0_{Di}\exp(-E_{Di}/k_BT), \tag{24}$$

where E_{Di} is the activation barrier for dissociation and ν^0_{Di} its frequency prefactor. The total frequency ν_{tot} of a diffusion event (DR or *mech*) is given by

$$\nu_{tot}=\nu^0_{mech}\exp(-E_{mech}/k_BT)+\nu^0_{Di}[1-P(0)]\exp(-E_{Di}/k_BT). \tag{25}$$

The total probability $P_{tot}(1)$ for a one-site move is given by

$$P_{tot}(1)=\{\nu^0_{mech}\exp(-E_{mech}/k_BT)+\nu^0_{Di}[1-P(0)]\times P^*(1)\exp(-E_{Di}/k_BT)\}/\nu_{tot}, \tag{26}$$

where the $P^*(k)$ are normalized on nonzero displacements

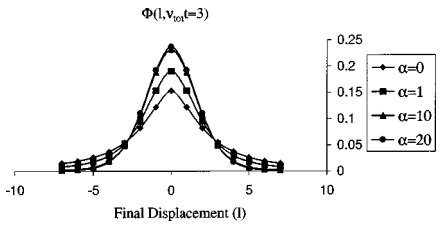

FIG. 7. Final-displacement probability distribution $\Phi(l,t)$ plotted for four different values of α, at a fixed time ($\nu_{tot}t=3$). Note that the curves for $\alpha=10$ (triangles) and for $\alpha=20$ (circles) are only slightly different, since the single-jump contribution is dominant. For small values of α, $\Phi(l,t)$ is much more spread out because of the long-jump contribution coming from the DR mechanism.

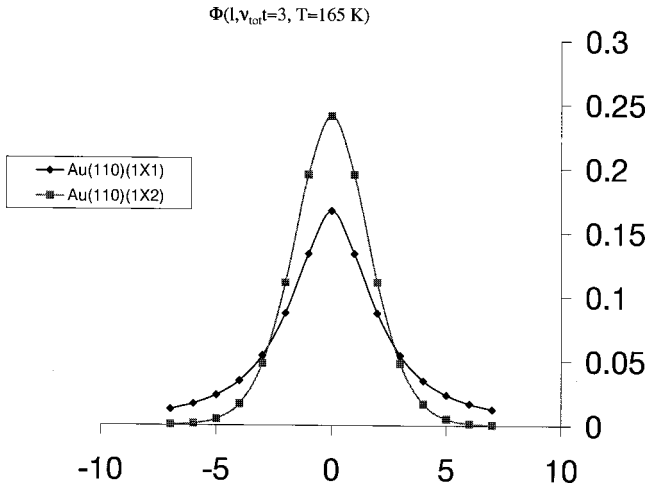

FIG. 8. Though the energy barriers are all of the same order, the opposite sign of $E_{mech}-E_{Di}$ [greater than 0 for $Au_2/Au(110)(1\times 2)$, less than 0 for $Au_2/Au(110)(1\times 1)$] causes a very different behavior of the two systems: indeed, $Au_2/Au(110)(1\times 1)$ follows the universal behavior, while $\Phi(l,t)$ for $Au_2/Au(110)(1\times 2)$ is a single-jump probability distribution. The two curves are computed for $T=165$ K, and $\nu_{tot}t=3$.

$$P^*(k)=\frac{P(|k|)}{1-P(0)}. \tag{27}$$

By defining α as

$$\alpha=\frac{\nu^0_{mech}}{\nu^0_{Di}[1-P(0)]}\exp[-(E_{mech}-E_{Di})/k_BT], \tag{28}$$

we find

$$P_{tot}(1)=\frac{\alpha+P^*(1)}{\alpha+1}. \tag{29}$$

For a k-sites jump ($k>1$), the total probability $P_{tot}(k)$ is

$$P_{tot}(k)=\frac{P^*(k)}{1+\alpha}. \tag{30}$$

Note that for every k, $P^*(k)$ is a universal number, given by Eqs. (5) and (27). Thus, if $P_{tot}(1)$ is experimentally determined in a direct way [as it seems to be possible for $Si_2/Si(001)$ (Ref. 14)], α is immediately found, by inverting Eq. (29)

$$\alpha=\frac{P_{tot}(1)-P^*(1)}{1-P_{tot}(1)}. \tag{31}$$

By making this measure at different temperatures, from the Arrhenius plot of α [Eq. (29)], it is possible to extract the energy difference $E_{CJ}-E_{Di}$. Note that α can be obtained by a final-displacement analysis as well: indeed for every k, $P_{tot}(k)$ only depends on α as a parameter. Equation (16) for the real system reads

$$\Phi(l,t)=\frac{1}{2\pi}\int_0^{2\pi}\cos(ql)\times\exp\left(-\nu_{tot}t\sum_{k>0}\{1-\cos(qk)\}P_{tot}(k)\right)dq. \tag{32}$$

For a given observation time t, once $\Phi(l,t)$ is experimentally determined, α can be found by fitting the data with Eq. (32). It is worth noticing that, in principle, once the energy difference (with the correct sign) $E_{mech}-E_{Di}$ is found, both energy barriers can be found by making a standard Arrhenius analysis of ν_{tot} at low temperatures, where the mechanism characterized by the lower energy barrier dominates. In Fig. 6 the deviations of $P_{tot}(k)$ from the universal behavior $P^*(k)$ are plotted as a function of $E_{mech}-E_{Di}$ at three different temperatures, assuming the same prefactor for both processes. The influence of α on the $\Phi(l,t)$ shape is investigated in Fig. 7 for a typical value $\nu_{tot}t=3$. Small values of α ($\alpha\rightarrow 0$) represent a system where dissociation dominates, while at large α, the single-jump contribution induced by the *mech* mechanism increases.

Let us now consider two explicit examples: gold dimers diffusion on both Au(110)(1×1) and Au(110)(1×2) surfaces. Following our MD results,[6] for the unreconstructed surface the dimer diffusion mechanism competing with DR is CJ, with $E_{CJ}=0.47$ eV, while $E_{Di}=0.45$ eV. On the missing-row geometry, there are two dimer diffusion mechanisms competing with DR: LF, with $E_{LF}=0.45$ eV, and CJ, with $E_{CJ}=0.52$ eV, while $E_{Di}=0.51$ eV. Up to now, we always considered only one diffusion mechanism competing with DR. The generalization to two different mechanisms *mech1* and *mech2* [CJ and LF for Au_2/Au(110)(1×2)] competing with DR is straightforward. Indeed, all the results we found in this section are still valid, if we generalize the definition of α to

$$\alpha=\frac{\nu^0_{mech1}\exp(-E_{mech1}/k_BT)+\nu^0_{mech2}\exp(-E_{mech2}/k_BT)}{\nu^0_{Di}\exp(-E_{Di}/k_BT)[1-P(0)]}. \tag{33}$$

For both systems the energy barriers are quite close, but in Au(110)(1×1) dissociation has the lowest barrier, while in Au(110)(1×2), LF is easier than dissociation. By using Eq. (32), where both frequency prefactors ($\nu^{1\times1}_{Di}=8$ ps^{-1}, $\nu^{1\times1}_{CJ}=5$ ps^{-1}, $\nu^{1\times2}_{Di}=4.7$ ps^{-1}, $\nu^{1\times2}_{CJ}=5.2$ ps^{-1}, $\nu^{1\times2}_{LF}=2.5$ ps^{-1}) and energy barriers are taken from our MD results, we obtain, for $T=165$ K, for an observation time $\nu_{tot}t=3$, the final-displacement curves shown in Fig. 8. The two curves are indeed qualitatively very different. For the missing-row reconstructed surface, $\Phi(l,t)$ is dominated by the single-jump contribution since α is large ($\alpha\approx60$). On the other hand, the unreconstructed surface almost displays the universal behavior since $\alpha\approx0.25$.

VI. CONCLUSIONS

In this paper we presented an analytical derivation for the long-jump probability distribution $P(|l|)$ induced by the DR mechanism on one-dimensional dimer diffusion. We showed that such probability distribution decays with the inverse of the jump length squared [for single adatoms, $P(|l|)$ decays exponentially]. Such law for the probability distribution can be experimentally checked both by direct atom-tracking and by a final-displacement analysis. In systems where DR is the dominant dimer-diffusion mechanism, this analysis leads to the determination of the dissociation rate and of the corresponding energy barrier. As demonstrated by MC simulations, even in presence of surface defects, $P(|l|)$ does not change significantly in a wide range of jump lengths $|l|$. In real systems, where DR is in competition with other dimer-diffusion mechanisms, deviations of the jump-length probability distribution from the universal law are connected with the activation-energy difference between DR and the other dimer-diffusion mechanism.

ACKNOWLEDGMENT

We acknowledge financial support from the Italian Ministero della Università e Ricerca under the project ''Dalle superfici ideali a quelle reali.''

*Electronic address: montalenti@fisica.unige.it

†Author to whom correspondence should be addressed. Electronic address: ferrando@fisica.unige.it

[1] J.A. Venables, G.D.T. Spiller, and M. Hanbucken, Rep. Prog. Phys. **47**, 399 (1984).

[2] K. Kyuno, A. Golzhauser, and G. Ehrlich, Surf. Sci. **397**, 191 (1998).

[3] B. Borovsky, M. Krueger, and E. Ganz, Phys. Rev. Lett. **78**, 4229 (1997).

[4] C.M. Goringe and D.R. Bauler, Phys. Rev. B **56**, R7073 (1997).

[5] T.R. Linderoth, S. Horch, L. Pedersen, S. Helveg, E. Laegsgaard, I. Stengsgaard, and F. Besenbacher, Phys. Rev. Lett. **82**, 1494 (1999).

[6] F. Montalenti and R. Ferrando, Phys. Rev. Lett. **82**, 1498 (1999).

[7] F. Montalenti and R. Ferrando, Surf. Sci. **432**, 27 (1999).

[8] T.R. Linderoth, S. Horch, E. Laegsgaard, I. Stensgaard, and F. Besenbacher, Surf. Sci. **402**, 308 (1998).

[9] P. Cowan and T.T. Tsong, Phys. Lett. A **53**, 383 (1975).

[10] T.T. Tsong, P. Cowan, and G. Kellogg, Thin Solid Films **25**, 97 (1975).

[11] P.J. Feibelman, Phys. Rev. Lett. **58**, 2766 (1997).

[12] G. Boisvert and L.J. Lewis, Phys. Rev. B **59**, 3946 (1999).

[13] W. Xu and J.B. Adams, Surf. Sci. **339**, 247 (1995).
[14] B. Borovsky, M. Krueger, and E. Ganz, Phys. Rev. B **59**, 1598 (1999).
[15] D. Hughes, *Random Walks and Random Environments* (Oxford Science, Oxford, U.K., 1995), Vol. 1.
[16] W.P. Pfluegl and R.J. Silbey, Phys. Rev. E **58**, 4128 (1998).
[17] M. Lovisa and G. Ehrlich, J. Phys. Colloq. **50**, C8-279 (1989).
[18] J. Ellis and J.P. Toennies, Phys. Rev. Lett. **70**, 2118 (1993).
[19] D. Cowell Senft, and G. Ehrlich, Phys. Rev. Lett. **74**, 294 (1995).
[20] T.R. Linderoth, S. Horch, E. Laegsgaard, I. Stensgaard, and F. Besenbacher, Phys. Rev. Lett. **78**, 4978 (1997).
[21] F. Montalenti and R. Ferrando, Phys. Rev. B **58**, 3617 (1998).
[22] F. Montalenti and R. Ferrando, Phys. Rev. B **59**, 5881 (1999).
[23] R. Ferrando, R. Spadacini, and G.E. Tommei, Phys. Rev. E **48**, 2437 (1993).
[24] V.I. Mel'nikov, Phys. Rep. **209**, 1 (1991).
[25] E. Hershkovitz, P. Talkner, E. Pollak, and Y. Georgievskii, Surf. Sci. **421**, 73 (1999).
[26] J.D. Wrigley, D.A. Reed, and G. Ehrlich, J. Chem. Phys. **67**, 781 (1977).
[27] K. Stolt, J.D. Wrigley, and G. Ehrlich, J. Chem. Phys. **69**, 1151 (1978).
[28] S.C. Wang, J.D. Wrigley, and G. Ehrlich, J. Chem. Phys. **91**, 5087 (1989).
[29] J.D. Wrigley, M.E. Twigg, and G. Ehrlich, J. Chem. Phys. **93**, 2885 (1990).